neurocritical care society Neurocrit Care (2011) 14:109–117
DOI 10.1007/s12028-010-9372-z

TRANSLATIONAL RESEARCH

# Recombinant Osteopontin Attenuates Brain Injury after Intracerebral Hemorrhage in Mice

**Bihua Wu · Qingyi Ma · Hidenori Suzuki · Chunhua Chen · Wenwu Liu · Jiping Tang · John Zhang**

Published online: 4 May 2010


**Abstract**
*Background* Osteopontin (OPN), an extracellular matrix glycoprotein, has been reported to inhibit inducible nitric oxide synthase (iNOS). We examined if recombinant OPN (r-OPN) inhibits iNOS and prevents brain injury in a mouse collagenase-induced intracerebral hemorrhage (ICH) model.
*Methods* One hundred one mice were randomly assigned to five groups: sham, ICH + vehicle, ICH + r-OPN (10, 50, or 100 ng per mouse) groups. Vehicle or r-OPN was administered via an intracerebroventricular infusion 20 min pre-ICH. Neurological scores and brain water content were evaluated at 24 and 72 h, and hemoglobin assay, Nissl staining and Western blot for iNOS, Stat1, matrix metalloproteinase (MMP)-9 and zonula occludens (ZO)-1 were performed at 24 h post-ICH.
*Results* r-OPN did not affect hematoma formation. Middle (50 ng)- and high (100 ng)-dose, but not low (10 ng)-dose of r-OPN treatment significantly improved neurological scores and brain water content compared with the vehicle group. The protective effect of r-OPN was associated with significantly rescued neuronal cells in the peri-hematoma region as well as a decrease in the Stat1 phosphorylation, iNOS induction, MMP-9 activation, and ZO-1 degradation.
*Conclusions* This study suggests that r-OPN may down-regulate iNOS expression by the inhibition of Stat1 phosphorylation, and therefore suppressing the MMP-9 activation, preventing ICH-induced brain injury in mice.

**Keywords** Brain edema · Collagenase · Intracerebral hemorrhage · Inducible nitric oxide synthase · Osteopontin

B. Wu · Q. Ma · H. Suzuki · C. Chen · W. Liu · J. Tang · J. Zhang
Department of Physiology and Pharmacology, Loma Linda University, Loma Linda, CA 92350, USA

J. Zhang
Department of Neurosurgery, Loma Linda University, Loma Linda, CA 92350, USA

J. Zhang
Department of Anesthesiology, Loma Linda University, Loma Linda, CA 92350, USA

B. Wu
Department of Neurology, Affiliated Hospital, North Sichuan Medical College, Nanchong City, Sichuan, China

J. Zhang (✉)
Department of Physiology, Loma Linda University School of Medicine, Risley Hall, Room 223, Loma Linda, CA 92354, USA
e-mail: johnzhang3910@yahoo.com

Spontaneous intracerebral hemorrhage (ICH) accounts for 10–15% of all stroke [1]. The mortality rate is high and most surviving patients retain a considerable functional handicap related to the specific site of ICH [1]. However, the data on the pathogenesis of ICH-induced brain injury are still limited, although matrix metalloproteinases (MMPs) have received special attention as contributors to brain damage produced by ICH [2]. A recent study showed that inducible nitric oxide synthase (iNOS) knockout mice had significantly less brain edema in a collagenase-induced ICH model [3]. Nitric oxide (NO) produced by iNOS is known to activate MMP-9 [2]. Thus, iNOS modulation might become a new therapy for ICH-induced brain injury.

Osteopontin (OPN) is a multifunctional extracellular matrix glycoprotein that has been linked to a variety of physiological and pathological processes in a wide range of

tissue [4–6]. In a mouse collagenase-induced ICH model, OPN was reported to be induced in infiltrated macrophages/activated microglia in the striatum surrounding the hematoma as well as in the hematoma and was suggested to be involved in the migration of neuroblasts: a few OPN-positive cells were detected at day 1, which were increased dramatically at day 3, and persisted from day 7 to day 28 after collagenase injection [7]. However, the role of OPN in an acute stage of ICH remains unknown. Since OPN has been shown to inhibit the iNOS induction in various tissues [8–11], we hypothesized that exogenous OPN may inhibit iNOS induction and therefore reduce brain injury after ICH. In this study, we examined the effects of recombinant OPN (r-OPN) on brain injury and the expression of iNOS and its related proteins in a mouse collagenase-induced ICH model.

## Materials and Methods

### Experimental Animals

All procedures for this study were approved by the Animal Care and Use Committee at Loma Linda University. One hundred one CD-1 mice, weighing 35–40 g, were randomly assigned to five groups: sham ($n = 27$), vehicle (ICH + saline, $n = 31$), low-dose (ICH + 10 ng of r-OPN/mice, $n = 6$), middle-dose (ICH + 50 ng of r-OPN/mice, $n = 27$), and high-dose (ICH + 100 ng of r-OPN/mice, $n = 10$) groups. Mice were housed in a 12-h light/12-h dark cycle in a specific pathogen-free facility with controlled temperature and humidity and were allowed free access to food and water. All neurological tests were performed during the light cycle.

### Mouse ICH Model

We produced the collagenase-induced ICH model as previously described [12]. Briefly, mice were anesthetized with an intraperitoneal injection of ketamine/xylazine (100/10 mg/kg), and positioned prone in a stereotactic head frame (Kopf Instruments, Tujunga, CA). An electronic thermostat-controlled warming blanket was used to maintain the core temperature at 37 ± 0.5°C. A cranial burr hole (1 mm) was drilled and a 27-gauge needle was inserted stereotactically into the right basal ganglia (coordinates: 0.9 mm posterior to the bregma, 1.5 mm lateral to the midline, and 4 mm below the dura mater). The collagenase (VII-S, Sigma; 0.05 U in 0.5 μL of saline) was infused into the brain at a rate of 0.25 μl/min with a microinfusion pump (Harvard Apparatus, Holliston, MA). Sham-operated mice were subjected to needle insertion only. The needle was left in place for an additional 10 min after injection to prevent possible leakage of the collagenase solution. After removal of the needle, the skull hole was closed with bone wax, the incision was closed with sutures, and the mice were allowed to recover. To avoid postsurgical dehydration, physiological saline was given to each mouse by subcutaneous injection in the amount of 2% of body weight immediately after surgery.

### Drug Administration and Intracerebroventricular Injections

Each dosage of r-OPN (EMD chemicals, La Jolla, CA) in 1 μl of sterile 0.9% saline was stereotactically injected into the right lateral ventricle (coordinates: 0 mm bregma, 1 mm lateral, and 2.5 mm ventral) using a 27-gauge needle 20 min before the induction of ICH [13]. The vehicle group was treated with the same volume of saline. The sham group was just inserted the needle.

### Neurobehavioral Tests

Neurological outcomes were assessed by a blinded observer just before euthanization at 24 and 72 h post-ICH, using a 21-point sensorimotor scoring system as per a previous report [14]. Briefly, the scoring system consisted of seven tests with scores of 1–3 for each test. These seven tests included: (i) spontaneous activity, (ii) symmetry in the movement of four limbs, (iii) forepaw outstretching, (iv) lateral turning, (v) climbing, (vi) body proprioception, and (vii) response to vibrissae touch. Higher scores indicate greater function.

For the corner turn test, a mouse was allowed to walk down a corridor into a 30° corner. To exit the corner, the animal could turn either to the right or left. The number of right and left turns out of 10 total attempts was recorded. The score was calculated as (number of left turns/total number of turns) × 100.

Wire hanging and beam balance tests were performed as previously described [15]. Bridges between platforms were built with wire (length, 50 cm; diameter, 1 mm) and beam (length, 90 cm; diameter, 1 cm). Mice were put on the center of the wire or beam and allowed to reach the platform. Mice were observed for both their time and behavior until they reached one platform and scored according to six grades. The test was repeated three times, and an average score was taken [minimum score = 0; maximum score (healthy mouse) = 5].

### Hemorrhage Volume

Hemoglobin assay was conducted as described previously [12]. Briefly, mice were killed with an overdose of isoflurane 24 h after ICH and transcardially perfused with

ice-cold phosphate-buffered saline (PBS). The ipsilateral hemisphere was homogenized for 60 s in a tube with distilled water (total volume 3 ml). After centrifugation, 400 µl Drabkin's reagent (Sigma–Aldrich, St. Louis, MO) was added to 100 µl aliquots of the supernatant and allowed to react for 15 min. The absorbance of this solution was read with a spectrophotometer (540 nm) and the amount of blood in each brain was calculated using a standard curve generated with known blood volumes.

### Brain Water Content

Brain water content was measured as previously described [16]. Briefly, mice were decapitated under deep anesthesia. Brains were immediately removed and divided into five parts: ipsilateral cerebral cortex, ipsilateral basal ganglia, contralateral cerebral cortex, contralateral basal ganglia, and cerebellum. The cerebellum was used as an internal control for brain water content. Tissue samples were weighed on an electronic analytical balance (APX-60, Denver Instrument) to the nearest 0.1 mg to obtain the wet weight (WW). The tissue was then dried at 100°C for 24 h to determine the dry weight (DW). Brain water content (%) was calculated as $[(WW - DW)/WW] \times 100$.

### Nissl Staining

At 24 h after ICH, mice were perfused under deep anesthesia with freezing PBS (pH 7.4), followed with 4% formalin. The brains were then removed and post-fixed in formalin at 4°C at least 3 days. Then the brain was dehydrated with 30% sucrose and the frozen coronal slices (10 µm thick) were sectioned in cryostat (LM3050S; Leica Microsystems, Bannockburn, IL). Nissl staining procedure using cresyl violet was applied. The number of neuron cells counted according to the morphology difference from 12 locations per mouse (three sections per mouse, four fields per section, microscopic field ×20) were averaged and expressed as the number of neurons per field.

### Western Blotting

Western blot analysis was performed as previously described [17, 18]. Briefly, the whole right cerebral hemispheres were homogenized, and aliquots were used to determine the protein concentration of each sample using a detergent compatible assay (Bio-Rad, Philadelphia, PA). Protein samples (50 µg) were loaded on a tris–glycine gel, electrophoresed, and transferred to a nitrocellulose membrane. Membranes were incubated overnight at 4°C with the primary antibodies: rabbit polyclonal anti-iNOS, goat polyclonal anti-Stat1, rabbit polyclonal anti-zonula occludens (ZO)-1, and rat monoclonal anti-MMP-9 antibodies (Santa Cruz Biotechnology, Santa Cruz, CA). Immunoblots were processed with secondary antibodies (Santa Cruz Biotechnology, Santa Cruz, CA) for 1 h at 21°C, probed, and then exposed to X-ray film. Blot bands were quantified using Image J software (NIH, Bethesda, MD). $\beta$-actin (Santa Cruz Biotechnology, Santa Cruz, CA) was blotted on the same membrane as a loading control.

### MMP Gelatin Zymography

The whole right cerebral hemispheres were homogenized in lysis buffer on ice. Homogenates were centrifuged, and total protein concentrations in the resulting supernatants were determined. For the MMP-9 zymography, we used a protocol published previously with modifications [19]. Briefly, equal amounts (50 µg) of total protein extracts were prepared and separated by 10% Tris–glycine gel with 0.1% gelatin as substrate (Bio-Rad). After separation, the gel was renatured and incubated with developing buffer at 37°C for 48 h. The gel was stained with 0.5% Coomassie blue R-250 for 60 min and then distained. Gelatinolytic activity was determined as clear zones or bands at the appropriate molecular weights. MMP-9 positive controls from Millipore (Temecula, CA) were used as standards.

### Statistical Analysis

A 21-point neurological score, wire hanging and beam balance tests were expressed as median ± 25th–75th percentiles, and were analyzed using Kruskal–Wallis test, followed by Steel–Dwass multiple comparisons. Other data were presented as mean ± SEM, and were analyzed with unpaired *t*-tests or one-way analysis of variance (ANOVA) followed by Tukey multiple comparison post-hoc analysis. A linear correlation was evaluated between the expression levels of protein in Western blots. $P < 0.05$ was considered statistically significant.

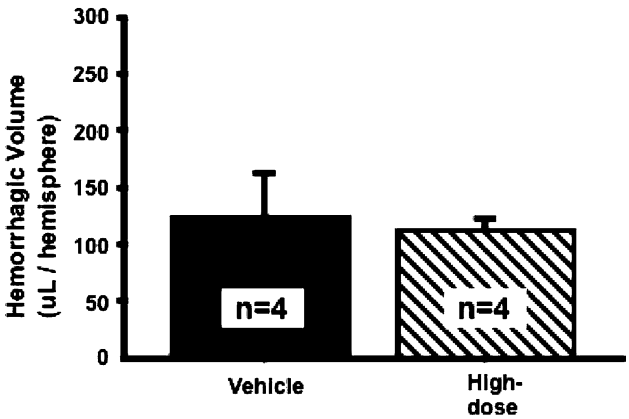


**Fig. 1** Hemorrhagic volume at 24 h post-ICH. There is no significant difference between the vehicle and high-dose r-OPN groups

## Results

### Hemorrhage Volume

There was no significant difference in hemorrhage volume between the vehicle and high-dose r-OPN groups at 24 h after ICH ($n = 4$ per group; Fig. 1), showing that intracerebroventricularly injected r-OPN had no effect on collagenase-induced hematoma formation.

### Neurobehavioral Test

No rats died in any groups after surgery. ICH caused significant neurobehavioral impairments as assessed by the

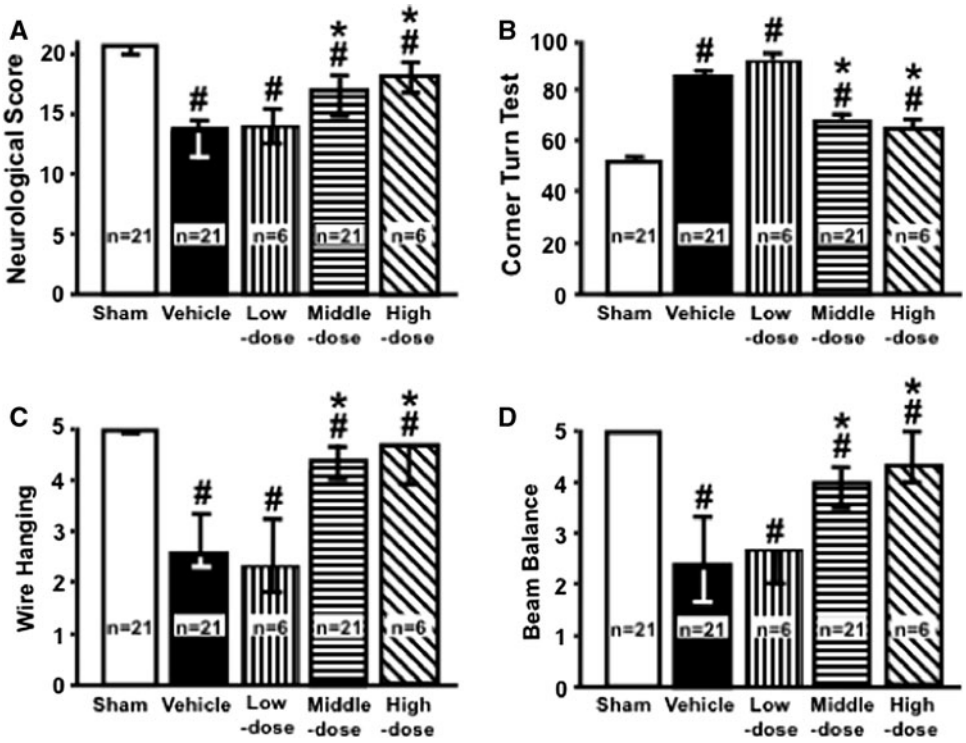


**Fig. 2** Neurobehavioral tests at 24 h post-ICH. **a** 21-point neurological score; **b** corner turn test; **c** wire hanging; **d** beam balance. Data are expressed as median ± 25th–75th percentiles (**a**, **c**, **d**) or mean ± SEM (**b**). Kruskal–Wallis test (**a**, **c**, **d**) or ANOVA (**b**), * $P < 0.05$ vs. vehicle group; # $P < 0.05$ vs. sham group

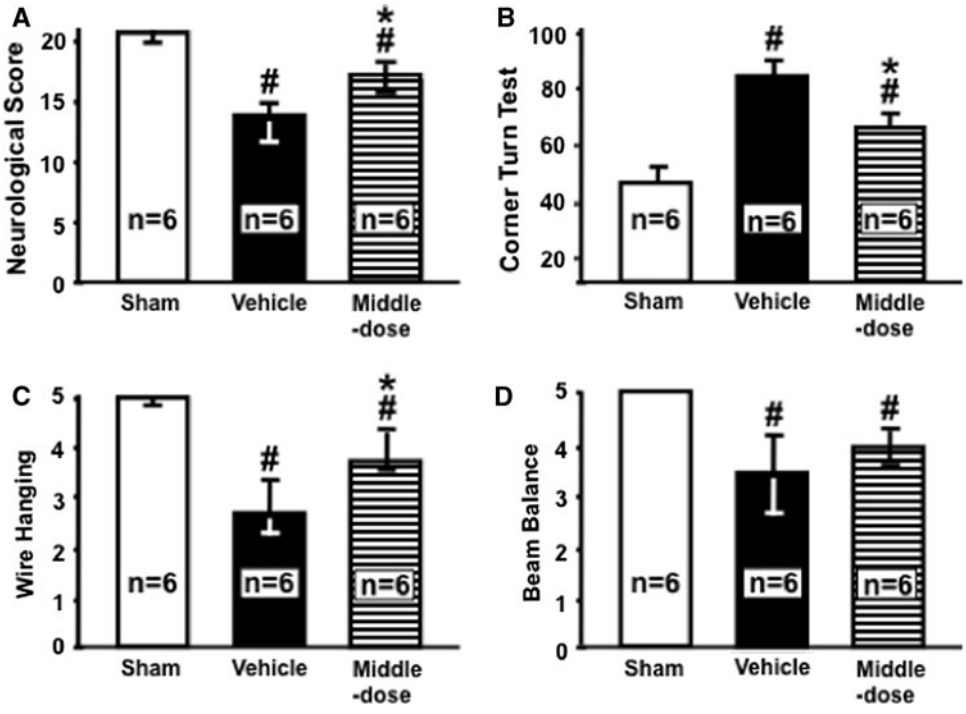


**Fig. 3** Neurobehavioral tests at 72 h post-ICH. **a** 21-point neurological score; **b** corner turn test; **c** wire hanging; **d** beam balance. Data are expressed as median ± 25th–75th percentiles (**a**, **c**, **d**) or mean ± SEM (**b**). Kruskal–Wallis test (**a**, **c**, **d**) or ANOVA (**b**), * $P < 0.05$ vs. vehicle group; # $P < 0.05$ vs. sham group

21-point scoring system, corner turn test, wire hanging and beam balance. Middle- ($n = 21$) and high-dose (n = 6), but not low-dose ($n = 6$) r-OPN treatment groups significantly prevented neurobehavioral impairments compared with the vehicle group ($n = 21$) at 24 h post-ICH ($P < 0.05$; Fig. 2). The neurobehavioral improvement by r-OPN (middle-dose, $n = 6$) was also observed at 72 h post-ICH ($P < 0.05$ vs. the vehicle group, $n = 6$; Fig. 3).

## Brain Water Content

ICH caused a significant increase in brain water content in the right (ICH-sided) cerebral cortex and basal ganglia at 24 h post-ICH (vehicle group, $n = 6$; Fig. 4a). Middle- and high-dose, but not low-dose r-OPN treatment groups ($n = 6$, respectively) significantly decreased the brain water content compared with the vehicle group ($P < 0.05$). The brain water content in the right cerebral cortex and basal ganglia in the vehicle group (n = 6) tended to increase at 72 h post-ICH (Fig. 4b). The r-OPN treatment (middle-dose, $n = 6$) also significantly decreased the brain water content compared with the vehicle group at 72 h post-ICH ($P < 0.05$).

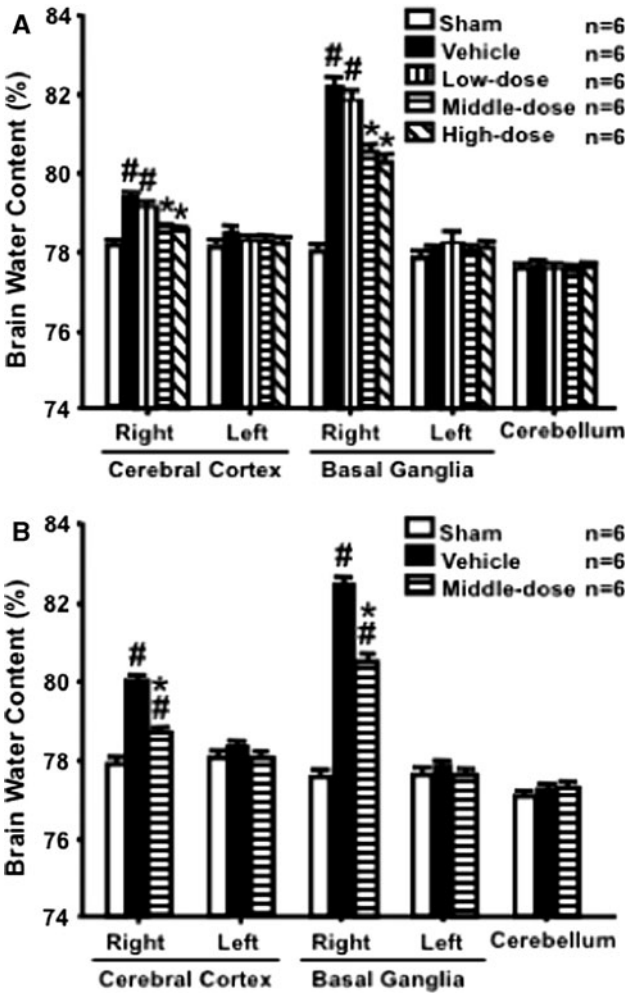


**Fig. 4** Brain water content at 24 (**a**) and 72 (**b**) h post-ICH. Data are expressed as mean ± SEM. ANOVA, * $P < 0.05$ vs. vehicle group; # $P < 0.05$ vs. sham group

## Neuronal Cell Counting

Middle-dose r-OPN treatment significantly rescued neuronal cells in the peri-hematoma region compared with the vehicle group ($P < 0.05$, $n = 3$ per group; Fig. 5).

## Effect of r-OPN on iNOS and Stat1

Western blot analysis showed that the level of iNOS in the right cerebral hemisphere was significantly higher in the vehicle group ($n = 6$) than in the sham group ($n = 6$) at 24 h post-ICH ($P < 0.01$; Fig. 6a). The middle-dose r-OPN treatment ($n = 6$) significantly reduced the expression of iNOS compared with the vehicle group ($P < 0.01$). The level of phosphorylated Stat1 was correlated with the iNOS level ($r = 0.876$, $P < 0.001$): the phosphorylated Stat1 increased significantly after ICH ($P < 0.01$) and was significantly decreased by the middle-dose r-OPN treatment at 24 h post-ICH ($P < 0.01$, $n = 6$ per group; Fig. 6b).

## Effect of r-OPN on MMP-9 and ZO-1

A significant increase in MMP-9 induction and activity was observed in the vehicle group ($n = 6$), and the middle-dose r-OPN treatment ($n = 6$) significantly inhibited the MMP-9 induction and activity compared with the vehicle group ($P < 0.05$; Figs. 7, 8a). The MMP-9 levels were correlated with the iNOS levels ($r = 0.896$, $P < 0.001$). ZO-1 was significantly degraded after ICH in the vehicle group compared with the sham group ($P < 0.05$), and the middle-dose r-OPN treatment significantly reduced the degradation of ZO-1 compared with the vehicle group ($P < 0.05$, $n = 6$ per group; Fig. 8b). The MMP-9 immunoreactivities had an inverse relation with the ZO-1 immunoreactivities, and the administration of r-OPN seemed to reverse these trends, with the conservation of ZO-1 immunoreactivities and marked reduction of MMP-9 immunoreactivities in the right cerebral hemisphere at 24 h post-ICH.

# Discussion

This study revealed that r-OPN prevented ICH-induced brain injury in terms of neurobehavioral tests, brain water content measurements, and neuronal cell counting in the

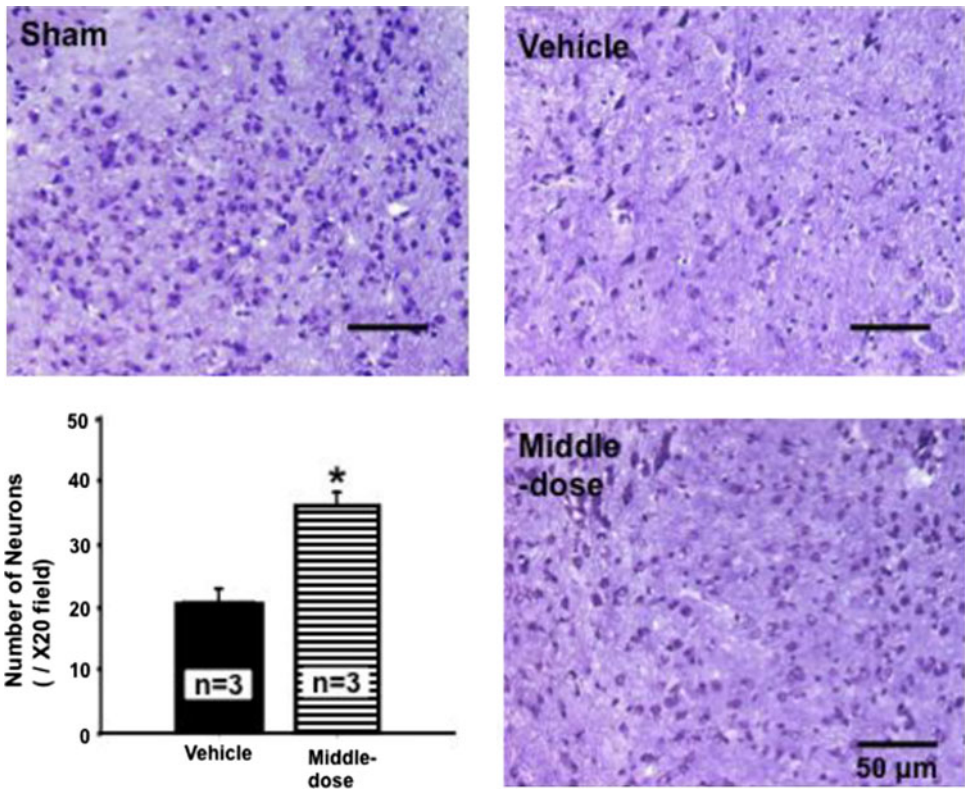


**Fig. 5** Neuronal cell counting in the peri-hematoma region at 24 h post-ICH. Data are expressed as mean ± SEM. Unpaired *t*-tests, * $P < 0.05$ vs. vehicle group

peri-hematoma region. The protective effects of r-OPN were associated with the inhibition of Sat1 phosphorylation, iNOS and MMP-9 induction, and the consequent preservation of tight junction protein ZO-1. This is the first study to demonstrate that r-OPN is protective for brain injury after ICH in mice.

The overproduction of NO by iNOS has been tightly linked to acute brain injury [20, 21]. The expression of iNOS is reported to be induced in the neutrophils, blood vessels, and astrocytes-like processes associated with the vessels in the peri-hematomal regions after an experimental ICH [22]. The neuroprotection by atorvastatin or bortezomib was associated with the inhibition of iNOS induction after ICH [23, 24]. Moreover, iNOS knockout mice had significantly less brain edema in a collagenase-induced ICH model [3]. The iNOS-derived NO can exert injurious effects by several mechanisms, one of which is the activation of MMP-9, causing neuroinflammation, cell death, and the blood–brain barrier (BBB) disruption [2, 25, 26]. The BBB is formed by specialized brain endothelial cells that are interconnected by tight junctions. ZO-1 is a peripheral tight junction protein that is found on the epithelial and endothelial cells membrane. Loss of ZO-1 from endothelial tight junction increases BBB permeability [27] and allows greater influx of blood-borne cells and substances into brain parenchyma, thus amplifying inflammation, leading to further parenchymal damage and edema formation [27].

OPN is a cell survival factor and may protect cells from tissue injuries via the multiple mechanisms [6, 13]. OPN exerts an anti-inflammatory effect by the downregulation of iNOS [4]. OPN is also reported to regulate the bioavailability of MMP-9 and provide the molecular link between degradation of the extracellular matrix and tissue remodeling [6, 28, 29]. Interestingly, OPN alone has no effect on iNOS activity or expression, nor does it affect MMP-9 activity and expression in various non-tumor culture cells [8, 29]. However, OPN inhibits iNOS expression and/or NO synthesis in mouse kidney epithelial cells, rat cardiac microvascular endothelial cells and myocytes, human macrophages, and isolated rat islets that are stimulated with proinflammatory cytokines plus lipopolysaccharide [8, 11, 30, 31]. Also, OPN is reported to inhibit proinflammatory cytokine-induced increase in activities and expression of MMP-9 in adult rat cardiac fibroblasts [2]. Consistent with these in vitro studies, our in vivo study showed that r-OPN prevented the ICH-induced increase in the expression of iNOS and MMP-9, and suppressed the degradation of ZO-1, reducing brain edema and improving neurobehavioral status in mice.

As the signaling pathways that are closely linked with iNOS expression, the nuclear factor (NF-$\kappa$B) transcription pathway, Janus tyrosine kinase/signal transducers and activators of transcription (JAK/STAT) pathway, and mitogen-activated protein kinases (MAPK) pathway are known [25]. Proinflammatory cytokines activate these

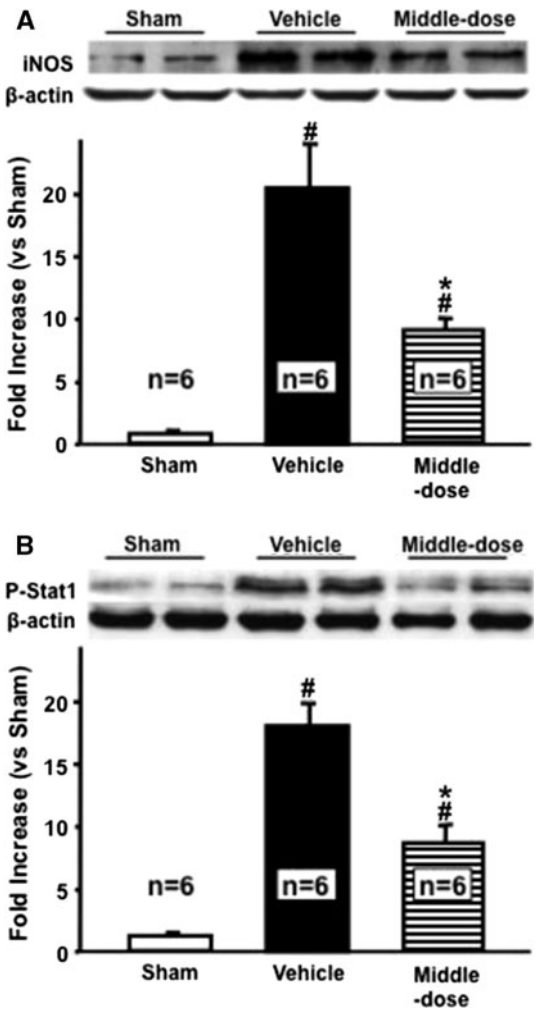


**Fig. 6** Western blots of iNOS (**a**) and phosphorylated Stat1 (P-Stat1; **b**) in the right cerebral hemisphere at 24 h post-ICH. The expression levels are expressed as a ratio of $\beta$-actin levels for normalization and as mean ± SEM. ANOVA, $^{\#}$ $P < 0.01$ vs. sham group; * $P < 0.01$ vs. vehicle group

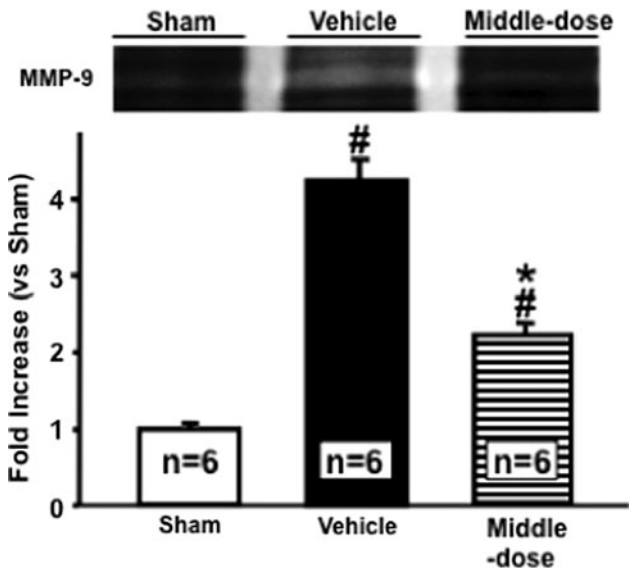


**Fig. 7** Gelatin zymograms of MMP-9 in the right cerebral hemisphere at 24 h post-ICH. The expression levels are expressed as a ratio of $\beta$-actin levels for normalization and as mean ± SEM. ANOVA, $^{\#}$ $P < 0.05$ vs. sham group; * $P < 0.05$ vs. vehicle group

pathways, and iNOS is induced in every tissue and organ system including brain [32]. A previous study showed that OPN provided protection against interleukin (IL)-1$\beta$-mediated cytotoxic effects by reducing IL-1$\beta$-induced NO production through the deactivation of NF-$\kappa$B activity in isolated rat islets [8]. Also, a recent study showed that OPN downregulated iNOS expression by accelerating ubiquitination and degradation of Stat1 in a murine sepsis model [33]. Stat1 is an essential activator of proinflammatory cytokine-mediated iNOS transcription [33]. However, no studies have reported if OPN can suppress MAPK activation. The NF-$\kappa$B and MAPK pathways, but not the JAK/STAT pathway, have been shown to be activated in an experimental ICH [22, 34]. This is the first to demonstrate that the JAK/STAT pathway is activated in a murine ICH model, in terms of Stat1 phosphorylation. Thus, we speculated that r-OPN suppressed the Stat1 phosphorylation and therefore inhibited the expression of iNOS, causing the inhibition of MMP-9 induction. To clarify other pleiotropic effects of r-OPN against ICH-induced brain injury, however, further investigations are needed.

This study had some limitations. First, it was not determined if r-OPN had effects on physiological parameters that affect brain injury, even though it has been already reported that the intracerebroventricular infusion of r-OPN had no effects on core temperature and blood glucose levels in a mouse middle cerebral artery occlusion model [35] and on blood pressure and blood gas in a rat subarachnoid hemorrhage model [6]. Second, the collagenase-induced ICH model used in this study is simple and reproducible, but has some weaknesses including more intense inflammatory reaction that bacterial collagenase by itself can elicit [36, 37]. As model differences may impact treatment efficacy, effects of r-OPN should be assessed in the blood injection model of ICH as well. Third, r-OPN was given via an intracerebroventricular injection as a pretreatment. This diminishes the translational significance of the study and should test the effects of post-treatment and other administration methods before clinical trials. Fourth, this study demonstrated the neuroprotective effects of r-OPN in an acute stage of ICH, but not the long-term effects. This is an important issue that should be addressed, even though r-OPN prevented neuronal injury in the perihematoma region 24 h post-ICH. Lastly, it remains unproved whether the post-ICH changes in various molecular markers (iNOS, Stat1, MMP-9, and ZO-1) and

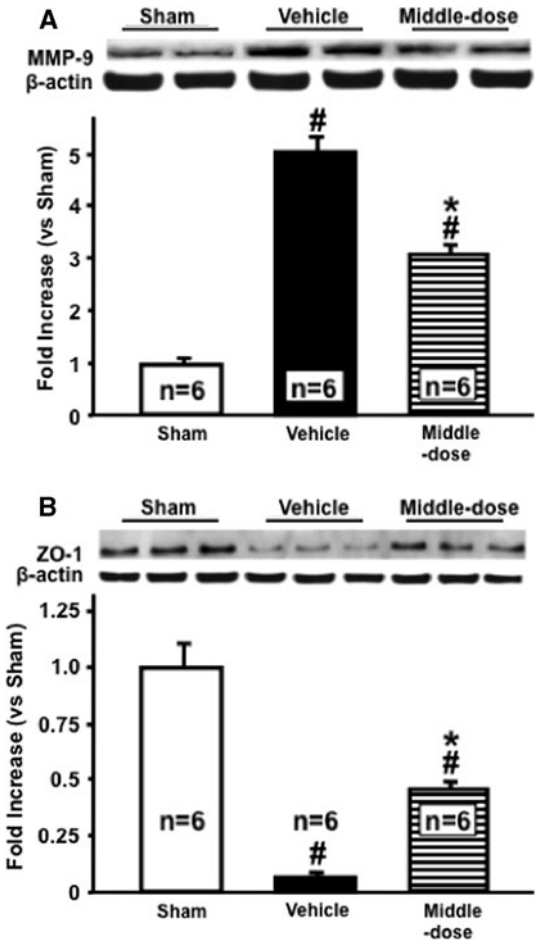


**Fig. 8** Western blots of MMP-9 (**a**) and ZO-1 (**b**) in the right cerebral hemisphere at 24 h post-ICH. The expression levels are expressed as a ratio of $\beta$-actin levels for normalization and as mean ± SEM. ANOVA, $^{\#}P < 0.05$ vs. sham group; $^{*}P < 0.05$ vs. vehicle group

the improvement by r-OPN in this study are merely epiphenomena or causative factors for ICH-induced brain injury and the underlying protective mechanism of r-OPN against it.

In conclusion, the findings in this study demonstrated that r-OPN is protective for ICH-induced brain injury in mice. r-OPN inhibited iNOS upregulation possibly via the inhibition of JAK/STAT pathway, resulting in a decrease in MMP-9 activity and the consequent preservation of tight junction protein ZO-1. The r-OPN treatment could be a new therapy for brain injury after ICH, and our findings warrant more research.

## References

1. Aronowski J, Hall CE. New horizons for primary intracerebral hemorrhage treatment: experience from preclinical studies. Neurol Res. 2005;27(3):268–79.
2. Xue M, Yong VW. Matrix metalloproteinases in intracerebral hemorrhage. Neurol Res. 2008;30(8):775–82.
3. Kim DW, Im SH, Kim JY, Kim DE, Oh GT, Jeong SW. Decreased brain edema after collagenase-induced intracerebral hemorrhage in mice lacking the inducible nitric oxide synthase gene. Laboratory investigation. J Neurosurg. 2009;111(5):995–1000.
4. Denhardt DT, Noda M, O'Regan AW, Pavlin D, Berman JS. Osteopontin as a means to cope with environmental insults: regulation of inflammation, tissue remodeling, and cell survival. J Clin Invest. 2001;107(9):1055–61.
5. Lee YJ, Park SJ, Lee WK, Ko JS, Kim HM. MG63 osteoblastic cell adhesion to the hydrophobic surface precoated with recombinant osteopontin fragments. Biomaterials. 2003;24(6):1059–66.
6. Suzuki H, Ayer R, Sugawara T, et al. Protective effects of recombinant osteopontin on early brain injury after subarachnoid hemorrhage in rats. Crit Care Med. 2010;38(2):612–8.
7. Yan YP, Lang BT, Vemuganti R, Dempsey RJ. Persistent migration of neuroblasts from the subventricular zone to the injured striatum mediated by osteopontin following intracerebral hemorrhage. J Neurochem. 2009;109(6):1624–35.
8. Arafat HA, Katakam AK, Chipitsyna G, et al. Osteopontin protects the islets and beta-cells from interleukin-1 beta-mediated cytotoxicity through negative feedback regulation of nitric oxide. Endocrinology. 2007;148(2):575–84.
9. Gao C, Guo H, Mi Z, Grusby MJ, Kuo PC. Osteopontin induces ubiquitin-dependent degradation of STAT1 in RAW264.7 murine macrophages. J Immunol. 2007;178(3):1870–81.
10. Scott JA, Weir ML, Wilson SM, Xuan JW, Chambers AF, McCormack DG. Osteopontin inhibits inducible nitric oxide synthase activity in rat vascular tissue. Am J Physiol. 1998;275((6 Pt 2)):H2258–65.
11. Singh K, Balligand JL, Fischer TA, Smith TW, Kelly RA. Glucocorticoids increase osteopontin expression in cardiac myocytes and microvascular endothelial cells. Role in regulation of inducible nitric oxide synthase. J Biol Chem. 1995;270(47):28471–8.
12. Tang J, Liu J, Zhou C, et al. Role of NADPH oxidase in the brain injury of intracerebral hemorrhage. J Neurochem. 2005;94(5):1342–50.
13. Doyle KP, Yang T, Lessov NS, et al. Nasal administration of osteopontin peptide mimetics confers neuroprotection in stroke. J Cereb Blood Flow Metab. 2008;28(6):1235–48.
14. Lo W, Bravo T, Jadhav V, Titova E, Zhang JH, Tang J. NADPH oxidase inhibition improves neurological outcomes in surgically-induced brain injury. Neurosci Lett. 2007;414(3):228–32.
15. Tsuchiyama R, Sozen T, Manaenko A, Zhang JH, Tang J. The effects of nicotinamide adenine dinucleotide on intracerebral hemorrhage-induced brain injury in mice. Neurol Res. 2009;31(2):179–82.
16. Tang J, Liu J, Zhou C, et al. Mmp-9 deficiency enhances collagenase-induced intracerebral hemorrhage and brain injury in mutant mice. J Cereb Blood Flow Metab. 2004;24(10):1133–45.
17. Chen W, Jadhav V, Tang J, Zhang JH. HIF-1alpha inhibition ameliorates neonatal brain injury in a rat pup hypoxic-ischemic model. Neurobiol Dis. 2008;31(3):433–41.
18. Ostrowski RP, Colohan AR, Zhang JH. Mechanisms of hyperbaric oxygen-induced neuroprotection in a rat model of subarachnoid hemorrhage. J Cereb Blood Flow Metab. 2005;25(5):554–71.
19. Lee CZ, Xue Z, Zhu Y, Yang GY, Young WL. Matrix metalloproteinase-9 inhibition attenuates vascular endothelial growth factor-induced intracerebral hemorrhage. Stroke. 2007;38(9):2563–8.
20. Pearse DD, Chatzipanteli K, Marcillo AE, Bunge MB, Dietrich WD. Comparison of iNOS inhibition by antisense and

pharmacological inhibitors after spinal cord injury. J Neuropathol Exp Neurol. 2003;62(11):1096–107.
21. Wada K, Chatzipanteli K, Kraydieh S, Busto R, Dietrich WD. Inducible nitric oxide synthase expression after traumatic brain injury and neuroprotection with aminoguanidine treatment in rats. Neurosurgery. 1998;43(6):1427–36.
22. Zhao X, Zhang Y, Strong R, Zhang J, Grotta JC, Aronowski J. Distinct patterns of intracerebral hemorrhage-induced alterations in NF-kappaB subunit, iNOS, and COX-2 expression. J Neurochem. 2007;101(3):652–63.
23. Jung KH, Chu K, Jeong SW, et al. HMG-CoA reductase inhibitor, atorvastatin, promotes sensorimotor recovery, suppressing acute inflammatory reaction after experimental intracerebral hemorrhage. Stroke. 2004;35(7):1744–9.
24. Sinn DI, Lee ST, Chu K, et al. Proteasomal inhibition in intracerebral hemorrhage: neuroprotective and anti-inflammatory effects of bortezomib. Neurosci Res. 2007;58(1):12–8.
25. Pannu R, Singh I. Pharmacological strategies for the regulation of inducible nitric oxide synthase: neurodegenerative versus neuroprotective mechanisms. Neurochem Int. 2006;49(2):170–82.
26. Tejima E, Zhao BQ, Tsuji K, et al. Astrocytic induction of matrix metalloproteinase-9 and edema in brain hemorrhage. J Cereb Blood Flow Metab. 2007;27(3):460–8.
27. Mahajan SD, Aalinkeel R, Sykes DE, et al. Tight junction regulation by morphine and HIV-1 tat modulates blood-brain barrier permeability. J Clin Immunol. 2008;28(5):528–41.
28. Rangaswami H, Bulbule A, Kundu GC. Osteopontin: role in cell signaling and cancer progression. Trends Cell Biol. 2006;16(2):79–87.
29. Xie Z, Singh M, Siwik DA, Joyner WL, Singh K. Osteopontin inhibits interleukin-1beta-stimulated increases in matrix metalloproteinase activity in adult rat cardiac fibroblasts: role of protein kinase C-zeta. J Biol Chem. 2003;278(49):48546–52.
30. Hwang SM, Lopez CA, Heck DE, et al. Osteopontin inhibits induction of nitric oxide synthase gene expression by inflammatory mediators in mouse kidney epithelial cells. J Biol Chem. 1994;269(1):711–5.
31. Rollo EE, Laskin DL, Denhardt DT. Osteopontin inhibits nitric oxide production and cytotoxicity by activated RAW264.7 macrophages. J Leukoc Biol. 1996;60(3):397–404.
32. Kilbourn RG, Traber DL, Szabo C. Nitric oxide and shock. Dis Mon. 1997;43(5):277–348.
33. Guo H, Wai PY, Mi Z, Gao C, Zhang J, Kuo PC. Osteopontin mediates Stat1 degradation to inhibit iNOS transcription in a cecal ligation and puncture model of sepsis. Surgery. 2008;144(2):182–8.
34. Wan S, Zhan R, Zheng S, Hua Y, Xi G. Activation of c-Jun-N-terminal kinase in a rat model of intracerebral hemorrhage: the role of iron. Neurosci Res. 2009;63(2):100–5.
35. Meller R, Stevens SL, Minami M, et al. Neuroprotection by osteopontin in stroke. J Cereb Blood Flow Metab. 2005;25(2):217–25.
36. James ML, Warner DS, Laskowitz DT. Preclinical models of intracerebral hemorrhage: a translational perspective. Neurocrit Care. 2008;9(1):139–52.
37. MacLellan CL, Silasi G, Poon CC, et al. Intracerebral hemorrhage models in rat: comparing collagenase to blood infusion. J Cereb Blood Flow Metab. 2008;28(3):516–25.